



Senescent cells enhance newt limb regeneration by promoting muscle dedifferentiation

Hannah E. Walters¹ | Konstantin E. Troyanovskiy^{1,2} | Alwin M. Graf¹ | Maximina H. Yun^{1,3,4}

¹Technische Universität Dresden, CRTD/Center for Regenerative Therapies Dresden, Dresden, Germany

²Freie Universität Berlin, Berlin, Germany

³Max Planck Institute for Molecular Cell Biology and Genetics, Dresden, Germany

⁴Cluster of Excellence Physics of Life, Technische Universität Dresden, Dresden, Germany

Correspondence

Hannah E. Walters and Maximina H. Yun, Technische Universität Dresden, CRTD/Center for Regenerative Therapies Dresden, Dresden, Germany.
Email: hannah.walters@mailbox.tu-dresden.de and maximina.yun@tu-dresden.de

Funding information

Deutsche Forschungsgemeinschaft, Grant/Award Number: 22137416, 450807335 and 497658823

Abstract

Salamanders are able to regenerate their entire limbs throughout lifespan, through a process that involves significant modulation of cellular plasticity. Limb regeneration is accompanied by the endogenous induction of cellular senescence, a state of irreversible cell cycle arrest associated with profound non-cell-autonomous consequences. While traditionally associated with detrimental physiological effects, here, we show that senescent cells can enhance newt limb regeneration. Through a lineage tracing approach, we demonstrate that exogenously derived senescent cells promote dedifferentiation of mature muscle tissue to generate regenerative progenitors. In a paradigm of newt myotube dedifferentiation, we uncover that senescent cells promote myotube cell cycle re-entry and reversal of muscle identity via secreted factors. Transcriptomic profiling and loss of function approaches identify the FGF-ERK signaling axis as a critical mediator of senescence-induced muscle dedifferentiation. While chronic senescence constrains muscle regeneration in physiological mammalian contexts, we thus highlight a beneficial role for cellular senescence as an important modulator of dedifferentiation, a key mechanism for regeneration of complex structures.

KEYWORDS

cellular senescence, dedifferentiation, ERK, FGF, regeneration, reprogramming, salamander, WNT

1 | INTRODUCTION

Cellular senescence is a highly dynamic, irreversible cell cycle arrest fate induced in response to the detection of potentially genotoxic stress (Campisi, 2013). Upon senescence induction, cells permanently exit the cell cycle, yet remain viable and metabolically active, exerting a strong influence over their microenvironment, most notably through the development of the senescence-associated secretory

phenotype ('SASP' [Acosta et al., 2008; Coppé et al., 2008; Kuilman et al., 2008]). Diverse physiological events can result in senescence induction, including oncogenic transformation, developmental cues organismal ageing and tissue injury. Nevertheless, key features of senescence including lysosomal dysfunction, resistance to apoptosis and acquisition of a secretory phenotype are largely conserved across physiological contexts and between species (Yun et al., 2015; Zhao et al., 2018).

Abbreviations: BMP, bone morphogenetic protein; CM, conditioned media; EdU, 5-ethynyl-2'-deoxyuridine; FCS, fetal calf serum; FGF, fibroblast growth factor; GFP, green fluorescent protein; MCK, muscle-specific creatine kinase; MT, myotube; MyHC, myosin heavy chain; PRO, proliferating; Rb, retinoblastoma; SA- β -gal, senescence-associated- β -galactosidase; SASP, senescence-associated secretory phenotype; SEN, senescent; YFP, yellow fluorescent protein.

This is an open access article under the terms of the [Creative Commons Attribution](https://creativecommons.org/licenses/by/4.0/) License, which permits use, distribution and reproduction in any medium, provided the original work is properly cited.

© 2023 The Authors. *Aging Cell* published by Anatomical Society and John Wiley & Sons Ltd.



Paradoxically, senescence induction can have beneficial or detrimental consequences in different contexts, depending on the nature of the senescence phenotype and the dynamics of senescent cell clearance (Walters & Yun, 2020). Cell senescence can drive tumour growth and age-related disease progression (Baker et al., 2016; Bussian et al., 2018; Childs et al., 2016; Jeon et al., 2017), yet it can also promote wound healing (Demaria et al., 2014; Jun & Lau, 2010), limit fibrosis (Kong et al., 2012; Krizhanovsky et al., 2008; Meyer et al., 2016) and coordinate organogenesis (Davaapil et al., 2016; Muñoz-Espín et al., 2013; Storer et al., 2013). Interestingly, senescence can impact two types of cellular plasticity of relevance to tissue renewal, namely reprogramming to pluripotency and stemness. Initially described as a cell-autonomous barrier to in vitro reprogramming (Banito et al., 2009), senescent cells can enhance this process in reprogrammable i4F mice by creating a tissue environment favourable to OSKM-mediated reprogramming via secreted factors (Mosteiro et al., 2016, 2018). Indeed, in the context of muscle regeneration, where a transient induction of senescence has been observed (Le Roux et al., 2015), additional senescent cells derived from irradiation or ageing enhance reprogramming in an i4F background (Chiche et al., 2017). Beyond reprogramming, transient exposure to oncogene-induced SASP fosters stemness in the mammalian liver and hair follicles, though extended exposure instead promotes paracrine senescence induction, limiting tissue renewal (Ritschka et al., 2017). Further, acquisition of stem cell features by senescent cells themselves has been reported in cancer contexts and proposed to drive tissue growth (Milanovic et al., 2018). These findings suggest that cell senescence could contribute to physiological regenerative processes, and that it may modulate other types of cellular plasticity.

Dedifferentiation, a process whereby terminally differentiated cells revert to a less differentiated state within their lineage, is central to the extensive regenerative abilities found in vertebrates such as salamanders and zebrafish (Cox et al., 2019; Gerber et al., 2018; Joven et al., 2019). Numerous cell types rely on dedifferentiation for the generation of regenerative progenitors in these organisms, with axolotl connective tissue (Gerber et al., 2018) and newt muscle (Wang & Simon, 2016) constituting noteworthy examples. In adult newts, limb loss triggers the formation of a blastema, a pool of lineage-restricted progenitors derived from both local stem cell activation and dedifferentiation events in mature cells from the stump, which undergoes expansion, re-differentiation and patterning to form a functional limb (Joven et al., 2019). Notably,

blastema formation is accompanied by the endogenous induction of senescent cells, which are present until the onset of differentiation and are subsequently cleared by a macrophage-dependent mechanism (Yun et al., 2015). Induction of senescence has subsequently been observed during zebrafish fin regeneration, where senolytic treatment slows regenerative outgrowth (Da Silva-Álvarez et al., 2020). These observations raise the possibility that cell senescence acts as a modulator of dedifferentiation, a key mechanism of appendage regeneration.

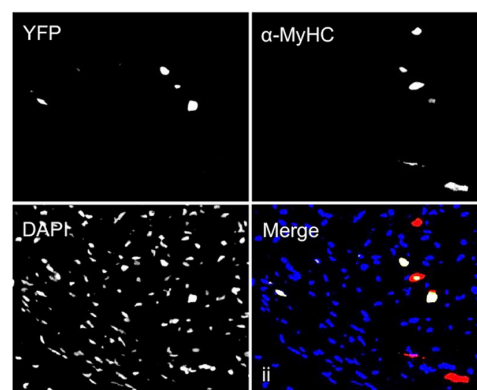
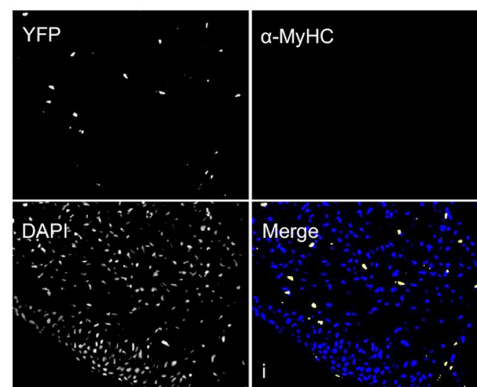
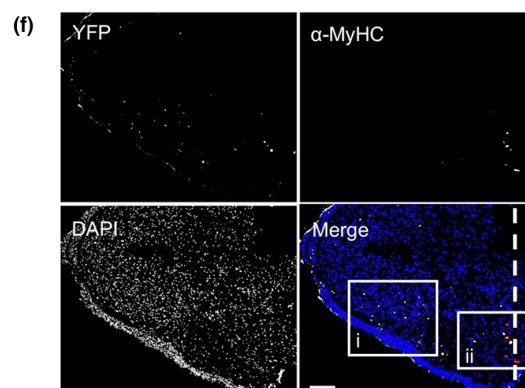
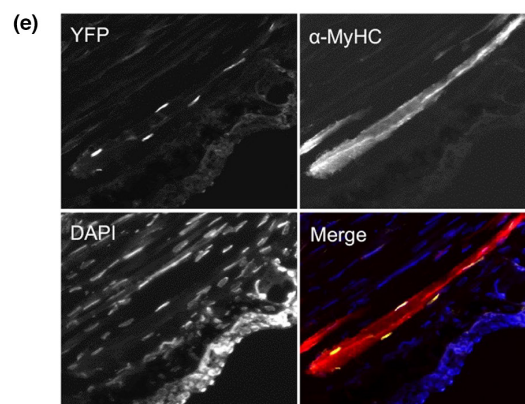
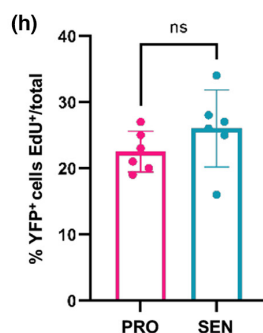
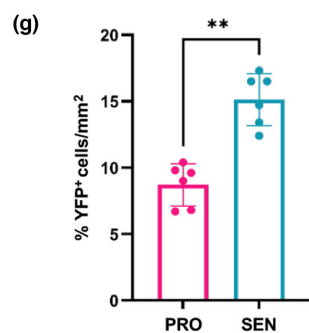
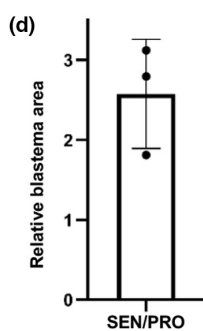
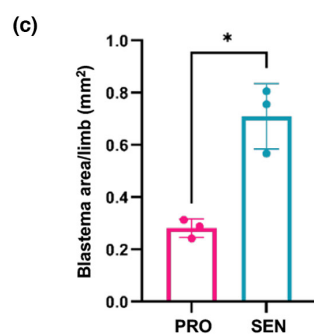
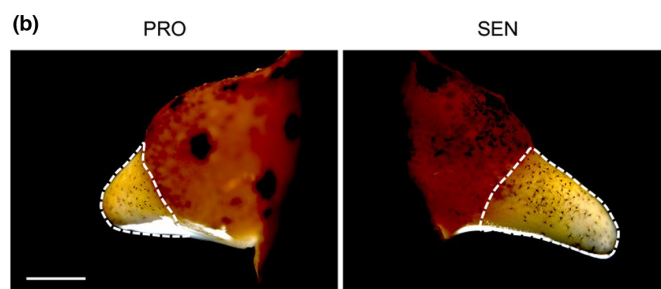
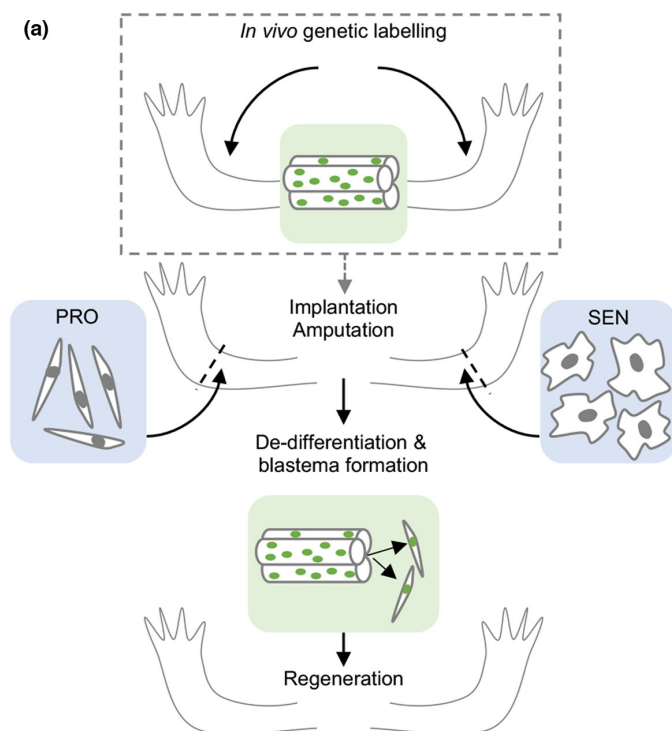
2 | RESULTS

2.1 | Implanted senescent cells accelerate blastema formation and promote myofibre dedifferentiation in vivo

During salamander limb regeneration, a robust and dynamic induction of endogenous cellular senescence occurs within the regenerating blastema and stump tissue. To investigate whether and how cellular senescence impacts on regenerative processes, we leveraged a system of exogenous senescent cell induction and implantation into *Notophthalmus viridescens* newt tissues (Yun et al., 2015). Limb mesenchyme-derived *N. viridescens* A1 cells were induced to undergo senescence upon DNA damage, which results in a phenotype that recapitulates many aspects of mammalian senescence including permanent cell cycle arrest, senescence-associated- β -galactosidase (SA- β -gal) activity, and SASP acquisition (Yun et al., 2015). Senescent or proliferating A1 cells were implanted into contralateral mature limb tissue of post-metamorphic newts, and the limbs subsequently amputated through the site of implantation to ensure implanted cells were present at the distal end of the remaining stump tissue (Figure 1a), the source of regenerative progenitors (Currie et al., 2016). Following amputation, limbs in which control proliferating cells were implanted reached a mid-bud blastema stage at 3 weeks post-amputation (Figure 1b). Strikingly, limbs in which senescent cells were implanted exhibited significantly larger blastema outgrowth, reaching a late-bud stage within the same period (Figure 1b–d), suggesting that exogenously derived senescent cells enhance blastema formation.

Given the importance of dedifferentiation for blastema formation, we hypothesised that senescent cells could serve as a temporary niche for

FIGURE 1 Senescent cells accelerate blastema formation and promote myofibre dedifferentiation in vivo. (a) Experimental schematic depicting fate-tracing and implantation approaches. (b–i) Senescent ('SEN') and control proliferating ('PRO') cells were generated in vitro and implanted into contralateral newt forelimbs, before amputation through the site of implantation. (b) Representative images of regenerating limbs at 18 days post-amputation (dpa). ($n=3$). Scale bar 1000 μ m. Blastema area is depicted by dashed lines. (c) Quantification of blastema area relative to limb width corresponding to (b). ($*p<0.05$, paired Student's t test, $n=3$). (d) Ratio of relative blastema area from (c) for the indicated conditions. (e–h) Effect of senescent cells on myofibre dedifferentiation. Myofibres were genetically labelled— (a), dashed square— prior to cell implantation and limb amputation. (e) Representative image of nucYFP-expressing nuclei within myofibres of the mature limb pre-amputation, as detected by α -GFP (yellow) and α -MyHC antibodies (red); nuclear counter-staining shown in blue. (f) Representative image of an 18dpa blastema, illustrating dedifferentiating nucYFP⁺/MyHC⁺ muscle fibres at the stump (ii) and their dedifferentiated, YFP⁺/MyHC⁺ mononucleate progeny (i). Scale bar 300 μ m. (g) Quantification of muscle-derived dedifferentiated progenitor cells (YFP⁺/MyHC⁺) in regenerating tissue at 18dpa, after implantation of senescent or proliferating cells. (h) Proliferation index of YFP⁺ cells in the regenerating limb for each condition as assessed by the proportion of YFP⁺ nuclei showing EdU incorporation. (g, h: $**p<0.01$, n.s. non-significant, paired student t test, $n=6$).





promoting dedifferentiation events, which could thus facilitate quicker blastema outgrowth. We tested this notion on the tractable system of muscle, a tissue known to regenerate via dedifferentiation of post-mitotic myofibres in adult newts (Sandoval-Guzmán et al., 2014; Tanaka et al., 1997). Upon amputation, myofibres undergo partial loss of muscle identity, cell cycle re-entry and fragmentation, generating mononucleate progenitors which proliferate, re-differentiate and fuse to form new myofibres (Wang & Simon, 2016). These progenitors can be identified through a well-established fate-tracing approach (Wang et al., 2015), where expression of a Cre recombinase under the control of a muscle-specific creatine kinase (MCK) promoter elicits nuclear YFP labelling of post-mitotic myofibre nuclei (Figure S1A). Through this approach, we genetically labelled muscle fibres in newt limbs to enable subsequent tracing of myogenic progenitors during regeneration, and repeated our implantation and amputation experiment (Figure 1a, Figure S1A).

Histological analysis showed successful labelling of mature limb myofibres as indicated by the expression of differentiation marker MyHC—Myosin Heavy Chain—(YFP⁺/MyHC⁺, Figure 1e, Figure S1B,C) and the appearance of YFP⁺/MyHC[−] mononucleate progenitor cells in the corresponding blastema mesenchyme (Figure 1f), which dynamically lose expression of muscle-specific genes such as myosin heavy chain (Figure 1f i and ii), reflecting dedifferentiation as previously demonstrated (Wang et al., 2015). Remarkably, senescent cell implantation led to a significant expansion of the pool of dedifferentiated YFP⁺/MyHC[−] progenitor cells in the regenerating tissue (Figure 1g, Figure S1D). Additionally, following the completion of regeneration, limbs in which senescent cells were implanted prior to amputation showed a significantly larger population of YFP⁺ nuclei within regenerated muscle fibres (MyHC⁺), consistent with enhanced initial dedifferentiation and subsequent redifferentiation towards muscle identity (Figure S1E,F).

The proportion of YFP⁺ cells incorporating EdU (injected at 14dpa) within the blastema mesenchyme, constituting dedifferentiated muscle progenitors, was not significantly altered (Figure 1h). These observations suggest that the senescence-dependent increase in dedifferentiated muscle progenitors is not driven by an enhancement of their proliferation capacity, but likely by the promotion of muscle dedifferentiation.

Together, these data suggest that the implantation of additional senescent cells during regeneration enhances muscle dedifferentiation, which may contribute to the observed acceleration of regeneration processes.

2.2 | Senescent cells promote dedifferentiation of newt myotubes through a paracrine mechanism

To more closely analyse the impact of senescent cells on muscle dedifferentiation, we employed an established newt myotube dedifferentiation paradigm. This system exploits the myogenic potential of the *N. viridescens* A1 cell line (Ferretti & Brookes, 1988), in which serum deprivation promotes cell cycle withdrawal and formation of multinucleate myotubes, which express muscle-related genes including

myosin heavy chain (MyHC), enabling their detection by immunostaining. Subsequently, certain culture conditions permit the analysis of dedifferentiation processes, including loss of differentiated cell identity, cell cycle re-entry from a terminally differentiated state and myotube fragmentation (Tanaka et al., 1997, 1999; Yun et al., 2013, 2014). Indeed, unlike terminally differentiated mammalian myotubes in which incorporated nuclei permanently exit the cell cycle, nuclei within newt myotubes retain the ability to respond to certain stimuli, and these dedifferentiation responses can be revealed by nucleotide analogue incorporation, highlighting nuclei traversing S-phase during dedifferentiation (Yun et al., 2014).

The capacity of A1 myotubes to dedifferentiate has been thoroughly demonstrated in vivo, where following injection with lineage tracers, implantation of purified myotubes into regenerating blastemas results in increasing populations of labelled mononucleate cells which undergo cell cycle re-entry subsequently found over time. These data indicate that implanted myotubes undergo dedifferentiation and generation of regenerative progenitors (Kumar et al., 2000; Lo et al., 1993). Thus, the A1 myotube paradigm faithfully recapitulates the muscle dedifferentiation events that occur during newt limb regeneration.

We first analysed whether senescence was itself induced during myotube dedifferentiation, as senescence induction can occur in response to cell fusion events, such as those elicited by viruses (Chuprin et al., 2013). To this end, we induced myotube formation through serum starvation (0.25% FCS), then elicited myotube dedifferentiation by re-exposure to 10% serum media and analysed senescence induction based on SA- β -gal activity (Figure S2). In contrast to control senescent cells, negligible SA- β -gal staining was observed in differentiated or dedifferentiated myotubes (Figure S2) where myotubes were revealed by α -MyHC immunostaining, and dedifferentiation was identified by MyHC⁺ myotubes exhibiting EdU incorporation (i.e., cell cycle re-entry), suggesting that senescence is not induced upon myogenic differentiation or dedifferentiation.

Next, we investigated whether senescent cells could contribute to myotube differentiation in a cell-autonomous manner, in two independent set-ups (Figure S3). Firstly, proliferating or senescent cells were seeded at high confluence and treated with differentiation media (0.25% FCS). Secondly, proliferating A1 cells were seeded into co-culture with senescent or control proliferating A1nGFP cells (constitutively expressing nuclear GFP [Yun et al., 2015]) under differentiation conditions. In both experimental set-ups, following 5-day exposure to differentiation media, we observed negligible formation of or contribution to myotubes from senescent cells (Figure S3), demonstrating that senescence induction constitutes a cell-autonomous barrier to differentiation in this context.

To test whether senescent cells promote myotube dedifferentiation, as suggested by our in vivo data (Figure 1), we generated myotubes in vitro, and co-cultured them with proliferating or senescent A1 cells. Subsequently, we quantified the proportion of myotube nuclei (MyHC⁺) undergoing cell cycle re-entry (EdU⁺) after 72h, as a quantifiable readout of dedifferentiation (Figure 2a). Importantly, co-culture with senescent cells resulted in an increase in myotube

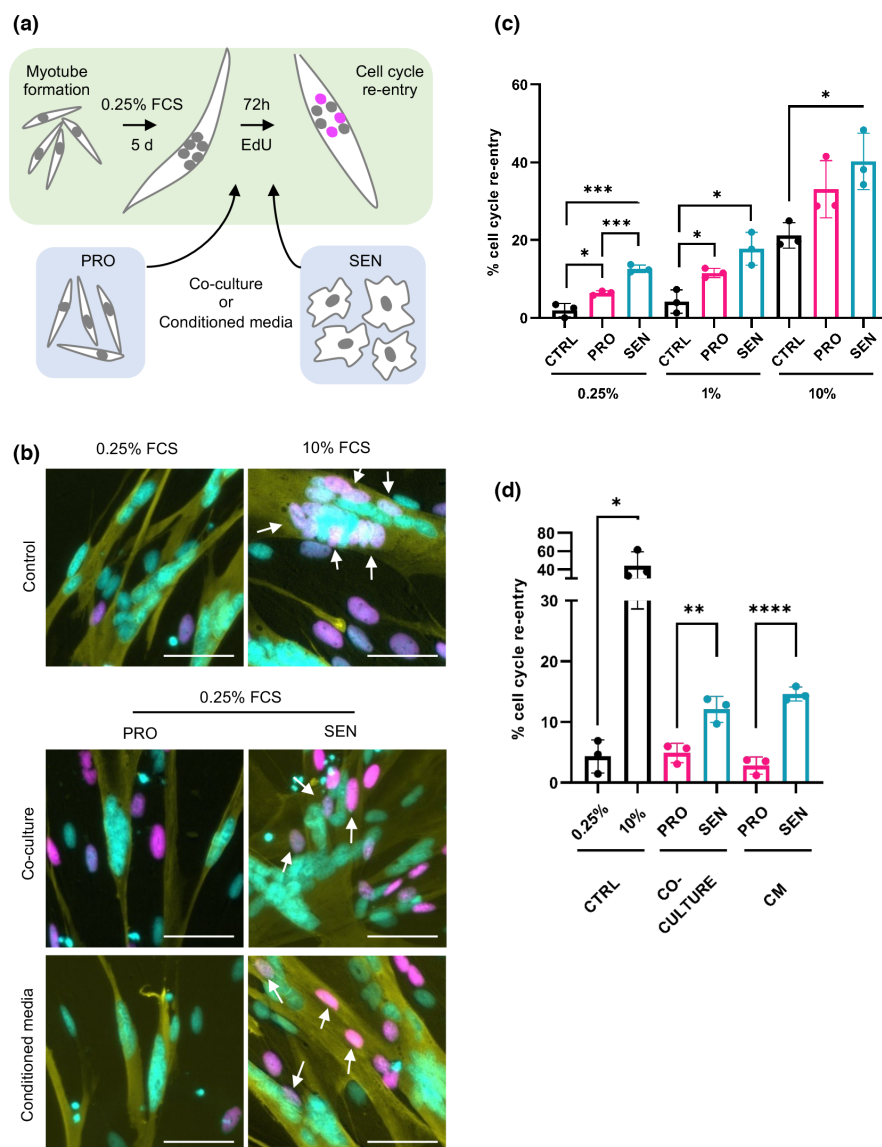
cell cycle re-entry compared to fresh media alone (Figure 2b,c), and a significant increase in cell cycle re-entry between proliferating and senescent cell co-culture under low serum conditions (0.25% FCS), suggesting that senescent cells can directly promote myotube dedifferentiation.

We next asked whether the viability of senescent cells is important for the observed cell cycle re-entry effects. Using a screening approach with proliferating or senescent cell viability as the readout, we identified ABT263 and dasatinib as selectively toxic to senescent A1 cells (Figure S4A,B). Using senolytic doses of either compound in our myotube co-culture set-up (1 μ M or 10 nM respectively), we observed that both senolytics ablate senescence-induced cell cycle re-entry (Figure S4C,D). Interestingly, while dasatinib has no effect on serum-induced cell cycle re-entry, treatment with the BCL2 inhibitor ABT263 alone enhances cell cycle re-entry downstream of serum exposure, consistent with a role of apoptotic signalling in dedifferentiation (Wang et al., 2015). Thus, these data show that senescent cell viability is critical for the promotion of myotube cell cycle re-entry in co-culture.

As senescent cells are known to influence their microenvironment largely through secretion of dynamic and heterogeneously expressed SASP factors, we next investigated whether senescence-induced cell cycle re-entry is mediated by soluble factors in a paracrine manner. Thus, we generated proliferating and senescent cell cultures and collected 48h conditioned media, which was filtered (0.22 μ m) and exposed to myotube cultures. After 72h treatment, we again analysed myotube cell cycle re-entry (Figure 2b,d), and observed a recapitulation of the effects of senescent cell co-culture, suggesting that senescence-induced cell cycle re-entry is mediated by secreted factors. Furthermore, using immunostaining, we observed that this effect is accompanied by increased phosphorylation of retinoblastoma (Rb) in myotube nuclei (Figure S5), a critical event in S-phase re-entry (Tanaka et al., 1997).

Given that many factors that induce dedifferentiation also promote general cell proliferation (Tanaka et al., 1997), we decided to further investigate whether senescent cells exert paracrine proliferative effects. As such, we exposed untreated, mononucleate A1 cells to conditioned media from proliferating or senescent cells

FIGURE 2 Senescent cells promote dedifferentiation of newt myotubes through a paracrine mechanism. (a) Schematic representation of the experimental set-up. (b) Representative images of myotubes following immunostaining against MyHC (yellow), EdU (magenta) and Hoechst (cyan) labelling. White arrows indicate EdU⁺ nuclei within myotubes. (c) Quantification of the proportion of myotube nuclei undergoing cell cycle re-entry for the indicated conditions, 72h post-treatment. PRO and SEN indicate co-culture with the respective cell populations. (d) Quantification of the proportion of myotube nuclei undergoing cell cycle re-entry for the indicated conditions, 72h post-treatment. Myotubes were co-cultured or treated with conditioned media derived from the indicated populations. Two-tailed unpaired student's *t* tests were used to compare data sets (**p* < 0.05, ***p* < 0.01, ****p* < 0.001 and *****p* < 0.0001).





(in 0.25% or 10% FCS), or control fresh media for 72h, then assessed proliferation rates by EdU incorporation. Indeed, we observed a small but significant increase in proliferation of mononucleate cells upon exposure to senescent CM in low serum, suggesting that factors secreted by senescent cells can exert pro-proliferative effects in mononucleate progenitor cells as well as in differentiated myotubes (Figure S6A).

We subsequently assessed whether senescent cells can also exert paracrine pro-proliferative effects in vivo, by implanting exogenously derived proliferating or senescent cells into mature newt limb tissue, then administering an 6h EdU pulse before sample collection (at 3dpi). Following histological analysis, we observed that cells in direct proximity to implanted senescent cells showed a higher rate of proliferation than those in which control cells were implanted (Figure S6B). Together, these data raise the hypothesis that senescence induction during regeneration may promote both muscle dedifferentiation and cellular proliferation in proximity.

2.3 | Transcriptomic insights into senescence-mediated dedifferentiation

To investigate the mechanistic basis for senescence-induced dedifferentiation, we performed bulk RNAseq analysis of proliferating (PRO) and senescent (SEN) A1 cells, as well as differentiated (MT_0.25%), serum-induced dedifferentiated (MT_10%) or conditioned media-exposed myotubes (MT_0.25%_PRO_CM and MT_0.25%_SEN_CM), each in triplicate (Figure 3a). Prior to RNA extraction, myotubes (MT) were collected by filtration to ensure analysis of pure populations. Following sequencing and alignment of reads to the *N. viridescens* transcriptome (Abdullayev et al., 2013), we observed widespread changes to the transcriptomic profile upon the induction of senescence, differentiation or dedifferentiation (Figure 3b). Distance analysis indicated a clear segregation between sample groups and strong similarity between replicates (Figure 3c). Notably, senescent CM-treated myotubes showed greater similarity to 10% FCS-treated myotubes than those treated with fresh 0.25% media or proliferating CM (Figure 3c).

Among the differentially regulated genes, the muscle stem cell and myoblast-associated transcription factor Myf5 showed robust expression in proliferating mononucleate cells, consistent with their myogenic potential, whereas this expression was significantly reduced in senescent cells (Figure 3d, Data S1), in line with the loss

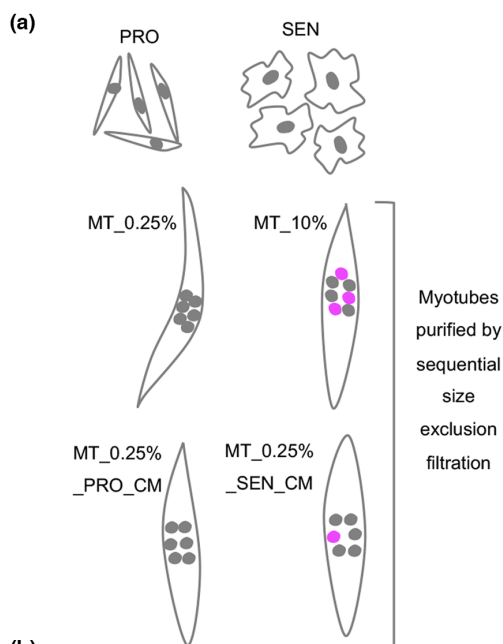
of myogenic capacity upon senescence induction. Similarly, Myf5 expression was downregulated upon differentiation, coincident with increased expression of myogenin, myosin isoforms and muscle-specific creatine kinase, indicating acquisition of differentiated myotube identity (Figure 3d, Data S1). Re-exposure of differentiated myotubes to serum and, to a lesser extent, senescent cell-derived factors, reduced these readouts of differentiated muscle identity (Figure 3d, Data S1). This supports the notion that senescence-derived secreted factors elicit muscle dedifferentiation.

As expected, markers of proliferation including cell cycle (e.g., CDKN1) and DNA replication-related (e.g., MCM7) transcripts were significantly reduced upon induction of senescence or differentiation (Figure 3e). Of note, expression of proliferation-related transcripts was increased in serum- or senescent cell CM-treated myotubes compared to their respective controls (Figure 3e), mirroring the increased myotube cell cycle re-entry observed in both contexts (Figure 2). In the senescence compartment, we noted the conservation of important senescence-associated transcriptional changes from mammalian systems, including upregulation of classical SASP factors including IL-6 and CSF1, as well as upregulation of several matrix-remodelling proteases (e.g., MMP3/10a, ADAM10L), DNA repair factors (e.g., LIG4) and reduction in expression of nuclear architecture transcripts including HMGB1 & 2, and Lamin B1 (Figure 3f). GO-term analysis of significantly enriched transcripts (Figure 3g, Data S2) underscored the loss of proliferative capacity upon senescence induction, where terms including 'DNA replication' and 'mitotic cell cycle' were associated with proliferating cell-enriched transcripts, and highlighted changes in RNA processing and ribosome assembly, mitochondrial and lipid metabolism upon senescence induction. Enrichment of intercellular communication-related terms (e.g., secretion, cell projection organisation), and changes related to MAPK and BMP networks were seen upon senescence induction. As expected, differentiation was associated with muscle related terms, calcium and MAPK signalling changes, while serum- and senescence-induced dedifferentiation were both associated with DNA replication, repair and cell cycle checkpoint-related terms.

2.4 | Senescent cells promote myotube cell cycle re-entry through the FGF-ERK signalling axis

To identify molecular mediators of senescence-induced cell cycle re-entry, we mined our RNAseq data set for candidates fulfilling

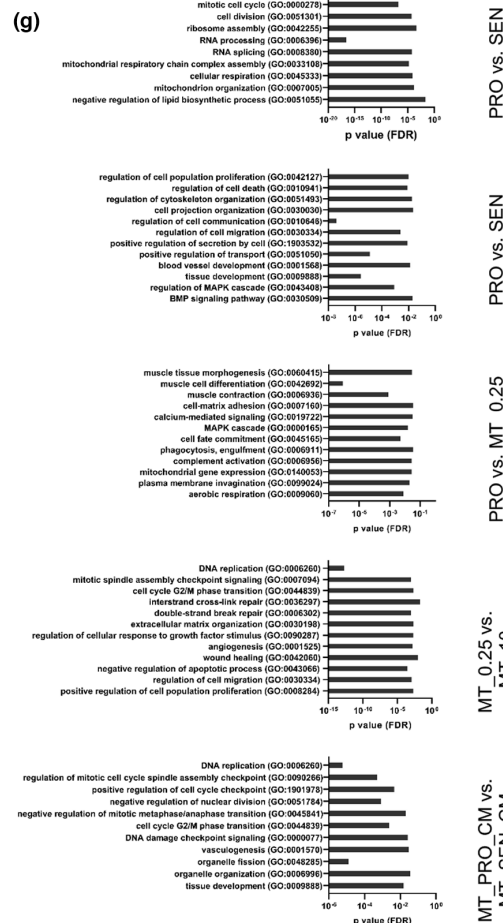
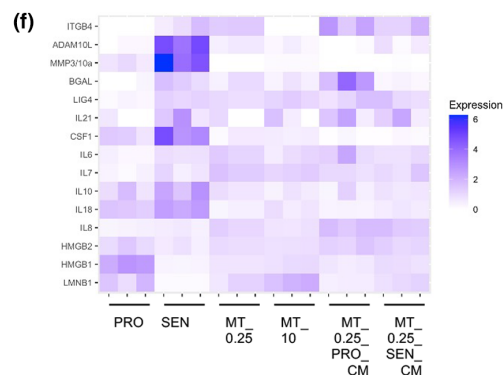
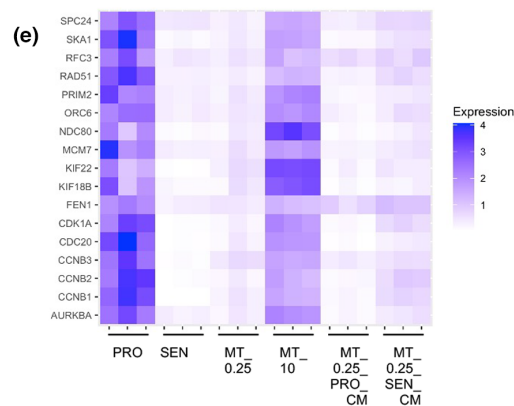
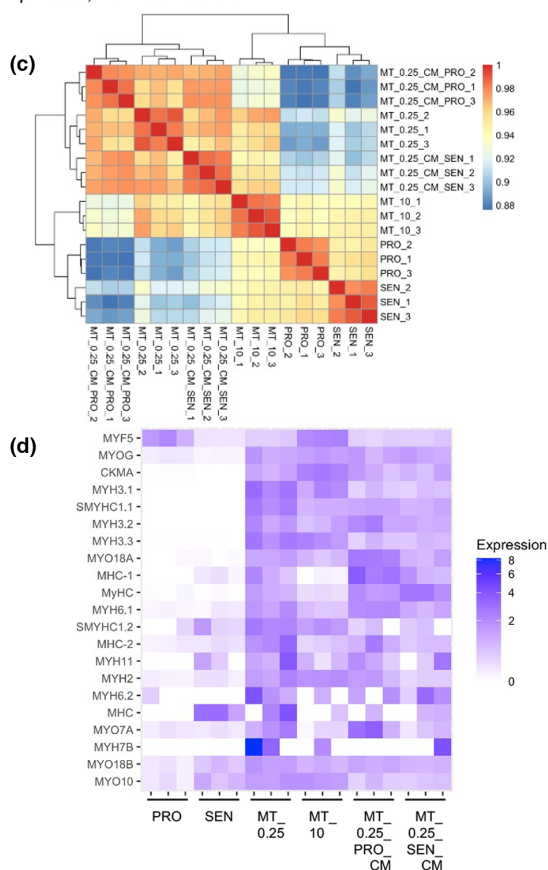
FIGURE 3 Transcriptomic insights into senescence-mediated dedifferentiation. (a) Experimental design schematic depicting sample groups for bulk RNAseq analysis (PRO: proliferating mononucleates, SEN: senescent cells, MT_0.25%: differentiated myotubes, MT_10%: serum-induced dedifferentiating myotubes, MT_0.25%_PROCM: myotubes cultured in proliferating cell conditioned media [0.25% FCS], MT_0.25%_SENCM: myotubes cultured in senescent cell conditioned media [0.25% FCS], all $n=3$). Dedifferentiating nuclei depicted in pink. (b) Comparison of significantly differentially regulated transcripts between sample groups. (c) Sample distance analysis plot. (d–f) Heat maps depicting differentiation (d), proliferation (e) and senescence (f)-related transcripts, with transcript expression for each replicate normalised relative to the mean reads per million transcripts across all sample groups. Data S3 contains tables with expression counts, log2fold change and adjusted p -values for each comparison. (g) GO-term analysis was performed using closest BLAST hits for transcripts significantly enriched (Log fold change >1 , $p < 0.05$) for the comparisons depicted (enriched population underlined).



(b)

Comparison	Transcripts mapped	LFC > 0	LFC < 0
PRO vs. SEN	27178	5958	5533
PRO vs. MT_0.25	27178	7783	8571
MT_0.25 vs. MT_10	27178	4773	4669
MT_0.25_PRO_CM vs. MT_0.25_SEN_CM	27178	1412	1109

$p = 0.05$, no LFC threshold





three criteria: they should constitute secreted factors, their expression should increase upon senescence induction and the cognate receptors and/or downstream signalling pathways for these factors should be expressed in myotubes undergoing dedifferentiation. As such, we identified several candidates belonging to the FGF, BMP, ERK and Wnt pathways, clotting factor protease activity and ECM remodelling factors (Figure S7). For each candidate pathway, we first assessed their general requirement for myotube cell cycle re-entry upon serum exposure (Figure 4a). We observed a strong suppression of cell cycle re-entry upon inhibition of BMP signalling using dorsomorphin (DMD), and MEK/ERK signalling using the inhibitor U0126 (Figure 4a), as previously observed (Wagner et al., 2017; Yun et al., 2014). Inhibition of protease activity using the broad-spectrum MMP inhibitor GM6001 or the serine protease inhibitor AEBF, active against clotting factor protease activity (Wagner et al., 2017), had little effect on serum-induced cell cycle re-entry (Figure 4a). In contrast, inhibition of Wnt (C59) or FGFR signalling (PD173074, AZD4547) led to moderate reductions in myotube cell cycle re-entry, with the strongest effect observed using the pan-FGFR inhibitor AZD4547 (Figure 4a).

We next tested the importance of these factors for senescence-induced cell cycle re-entry (Figure 4b). Blocking BMP or ERK signalling abrogated serum-induced cell cycle re-entry (Figure 4b). Senescence-induced cell cycle re-entry is likely to rely on ERK signalling within dedifferentiating myotubes to coordinate cell cycle re-entry, in the light of previous work (Yun et al., 2014). Further, soluble BMP factors have been shown to promote cell cycle re-entry (Wagner et al., 2017), though intriguingly, we observed notably larger myotubes following DMD treatment, suggesting a possible role for the inhibition of BMP signalling in facilitating myogenic differentiation. Indeed, we observed increased myogenesis of A1 cells in high serum medium upon treatment with 1 μ M DMD (Figure S8). These data suggest an additional role for BMP signalling in myogenic differentiation, and are consistent with previous reports examining BMP inhibition in C2C12 murine in vitro myogenesis (Horbelt et al., 2015). It is thus likely that BMP inhibition promotes differentiation and blocks dedifferentiation irrespective of stimuli derived from serum or senescent cells.

While protease inhibition had no effect on senescence-induced cell cycle re-entry (Figure 4b), inhibition of Wnt signalling decreased the effect of senescent cell co-culture and abrogated that of senescent CM (Figure 4b), suggesting that WNT ligands contribute to this process. Further, inhibiting FGFR signalling using PD173074 (FGFR1)

or AZD4547 (FGFR1-3) resulted in the blockage of senescence-induced cell cycle re-entry by co-culture or CM, suggesting a critical role of FGF signalling in mediating this process (Figure 4b).

We further investigated the hypothesis that the effects of senescent cells are mediated through the FGF signalling axis using small molecule agonists. We identified a BMP agonist (sb4, BMP4), a Wnt signalling agonist ('Wnt agonist') and an FGFR1 agonist (SUN11602). After initial toxicity screening (data not shown), we exposed myotubes to a dose range of each agonist, in fresh control or proliferating/senescent cell-conditioned media as before. Intriguingly, we observed no increase in cell cycle re-entry under any conditions with either the BMP agonist sb4 or the Wnt agonist, but upon treatment with the FGFR1 agonist SUN11602, we observed a dose-dependent increase in cell cycle re-entry in all conditions, apart from exposure to senescent cell-conditioned media (Figure S9). These data not only suggest that activating FGFR1 signalling boosts cell cycle re-entry in myotubes, but that FGFR1 activation may be saturated by senescent cell exposure in our experimental settings.

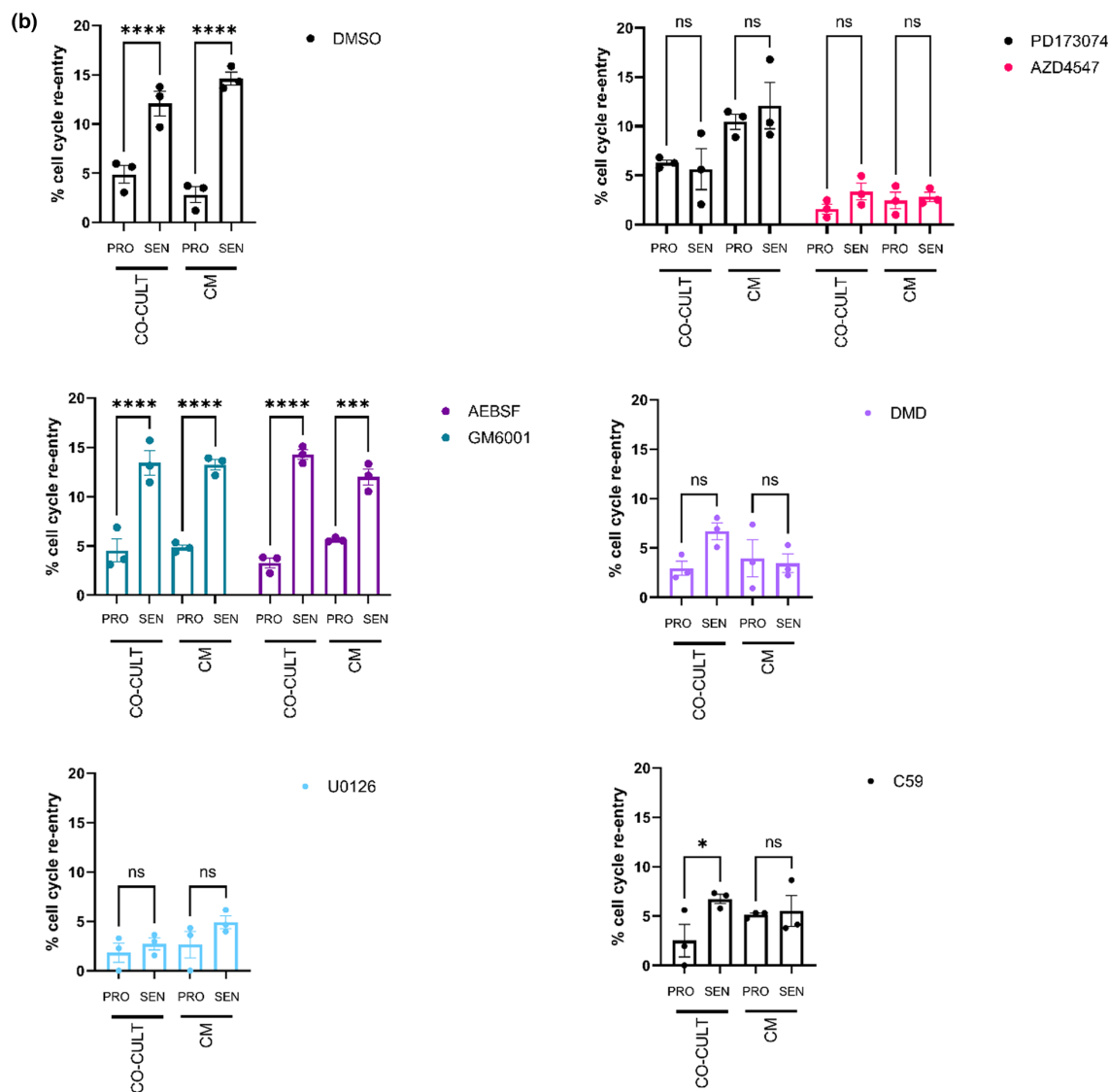
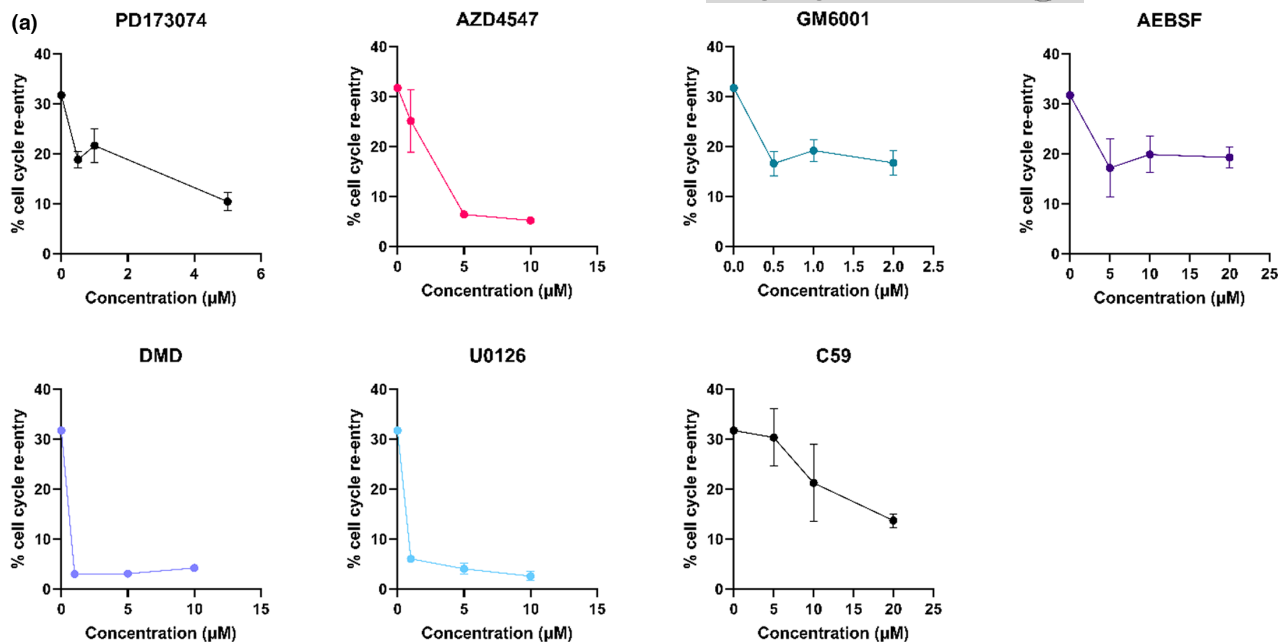
Given the upregulation of secreted FGF ligands in senescent cells, the robust expression of FGF receptors in dedifferentiating myotubes (Figure S7), as well as the critical role of the FGF-effector ERK in cell cycle re-entry (Figure 4), the FGF-ERK axis emerges as a direct mediator of senescence-induced cell cycle re-entry (Figure S10).

3 | DISCUSSION

This study demonstrates that cellular senescence can play beneficial roles during salamander limb regeneration. Specifically, we show that implanted senescent cells enhance muscle dedifferentiation, a critical process underlying successful limb regeneration, and uncover that they are able to modulate muscle dedifferentiation directly, through the secretion of paracrine factors including WNT and FGF ligands.

As such, our findings provide important advances for our understanding of senescent cell functions as well as early events during limb regeneration, opening up several research avenues. With regards to limb regeneration, the development of in vivo senescent cell labelling and depletion approaches in newt species should enable in-depth explorations of the physiological functions of these significant cellular players in the future. In addition, as dedifferentiation has been shown to underlie axolotl connective tissue regeneration (Gerber et al., 2018), it would be of interest to assess if senescent cells modulate this process. Further, probing the impact of senescent

FIGURE 4 Senescent cells promote cell cycle re-entry through the FGF-ERK signalling axis. (a, b) Quantification of the proportion of myotubes undergoing cell cycle re-entry for the indicated conditions, 72 h post-treatment. Myotubes were generated and subsequently exposed to DMSO vehicle control or inhibitors in 10% (a) or 0.25% (b) FCS in the presence of proliferating/senescent cell co-culture or conditioned media treatment. In (a), inhibitors were used over a non-toxic dose range. In (b), inhibitors were used at the following concentrations: PD173074 1 μ M, AZD4547 5 μ M, GM6001 2 μ M, AEBF 20 μ M, U0126 10 μ M, DMD 1 μ M and C59 10 μ M. Cell cycle re-entry was quantified as the proportion of myotube (MyHC⁺) nuclei showing EdU incorporation. Statistical analysis was performed using two-way ANOVA and Tukey post hoc multiple comparisons testing (* p < 0.05, ** p < 0.01, *** p < 0.001 and **** p < 0.0001, ns: not significant). Representative data from $n > 2$ experiments are shown. In (b), statistical comparisons between co-culture (PRO vs SEN) and conditioned media (PRO vs. SEN) in each inhibitor are shown, and full statistical analysis between inhibitors and DMSO treatment is detailed in Data S4.





cells on transdifferentiation, as it happens in the salamander lens (Tsonis, 2006), will be relevant for understanding their roles in different plasticity contexts.

It remains likely that senescent cells play additional roles during salamander limb regeneration. Indeed, our data suggest that these cells can promote cell proliferation in vitro and in vivo (Figure S6). While we have not observed sustained, pro-proliferative effects specific to the muscle progenitors in the blastema (Figure 1h), it remains conceivable that senescent cells promote proliferation of additional blastema populations, which may explain the notable acceleration of blastema development observed upon senescent cell implantation (Figure 1b–d). This is in agreement with further data from our group (Yu et al., 2022), which reports that senescent cells facilitate progenitor cell expansion in the axolotl. Additionally, senescent cell clearance in salamanders is achieved by macrophages (Yun et al., 2015), raising the possibility that senescent cells may have indirect functions via recruitment or regulation of immune cell activity, important in other regenerative contexts (Ratnayake et al., 2021). Lastly, the immune-dependent clearance mechanism acting in salamanders may be critical to ensure that senescence induction has beneficial rather than detrimental consequences, limiting cell senescence to a short time-window following injury and thus creating a transient niche permissive to dedifferentiation.

FGF signalling stands out as a key mediator of senescence-induced dedifferentiation (Figure 4). In agreement, chemical approaches suggest FGFR1 activity is central for dorsal iris pigment epithelial cell dedifferentiation during newt lens regeneration (Del Rio-Tsonis et al., 1998), and for blastema formation in the zebrafish fin (Poss et al., 2000). Similarly, the coordinated activity of FGF and BMP signalling—originating from the dorsal root ganglia—contributes to blastema formation in axolotl limb regeneration (Satoh et al., 2016). Highlighting the evolutionary conservation of pro-regenerative roles of FGF ligands, FGF4 promotes limb outgrowth in chicken (Kostakopoulou et al., 1996), while FGF2 is upregulated during blastema growth in murine digit tip regeneration (Takeo et al., 2013). Further careful analysis will be required to elucidate which of the senescence-upregulated newt FGF ligands is responsible for the promotion of dedifferentiation in this context. Additionally, our work uncovers WNT factors as contributors to the cell cycle re-entry effect. How WNT and FGF pathways interact to promote dedifferentiation warrants further investigation.

Together, our findings uncover a beneficial role for cellular senescence during newt limb regeneration through the non-cell-autonomous promotion of muscle dedifferentiation. In contrast, chronic senescence constrains muscle regeneration in physiological mammalian contexts (García-Prat et al., 2016). In light of our data, examination of cross-species differences in senescent cell nature, senescent-progenitor and immune crosstalk at the site of injury, and dynamics of senescence induction and clearance, could be instructive for limiting the deleterious effects of senescent cells in mammals and harnessing their beneficial traits in clinical settings.

3.1 | Limitations of the study

Due to the technical limitations of working with *N. viridescens* newts, we have been unable to assess the nature and possible roles of endogenous senescent cells during newt limb regeneration. The conservation of characteristics between in vitro and in vivo senescent cells remains a key area of interest in the senescence field and will be critical for future investigation.

4 | METHODS

4.1 | Animal procedures

Procedures for care and manipulation of *N. viridescens* newts used in this study were carried out in compliance with the Animals (Scientific Procedures) Act 1986, approved by the United Kingdom Home Office. Animals were maintained in individual aquaria at ~18–20°C, as previously described.

Tracing of dedifferentiated progenitor cells was performed as described (Wang et al., 2015) with the following modifications: plasmids (MCK:Cre, CMV:Tol2-transposase; CAG:loxP-cherry-stop-loxP-h2bYFP) were purified by caesium chloride preparation. Electroporations were carried out using a SD9 Stimulator device as previously described (Yun et al., 2013).

For cell implantation, senescent and control proliferating cells were generated as below. Newts were anaesthetised in 0.1% tricaine and 2000 cells were subsequently implanted into contralateral limbs using 10 µL Hamilton syringe (Hamilton) with a 30^{1/2} g, 45° tip needle (Hamilton) attached to a micromanipulator, using Fast Green to track the distribution of cell solution within the tissues, as described (Yun et al., 2015). Implantations were carried out under a Zeiss Axiozoom V.16 fluorescence stereomicroscope and cells were implanted along electroporated area based on fluorescence. Newts were amputated at the mid-humerus level through the site of cell implantation/tissue electroporation under a Zeiss Axiozoom V.16 fluorescence stereomicroscope. Animals were allowed to regenerate at 20°C. To detect EdU incorporation, 10 mM EdU (20 µL per animal) were administered by intraperitoneal injection. Tissues were subsequently collected and processed as described below.

4.2 | Tissue sectioning and histology

For analysis of dedifferentiation, regenerating limbs were collected by amputation and fixed in 4% (wt/vol) ice-cold paraformaldehyde (PFA) for 16–18 h at 4°C, washed twice in PBS and embedded in Tissue Tek-II. The samples were sectioned longitudinally in a cryostat at 10 µm. Sections were collected in Superfrost slides and stored at –20°C. Antibody staining of tissue sections was performed using standard protocols with the indicated antibodies (Table S2). EdU incorporation was determined subsequent to immunostaining



with anti-YFP antibodies using Click-iT Edu Alexa Fluor 594 Imaging kit (Life Technologies). For analysis of dedifferentiation, for each sample, the number of YFP⁺/MHC⁺ cells in the blastema was normalised relative to the number of labelled YFP⁺ myonuclei in the stump (YFP⁺/MHC⁺).

4.3 | Cell culture

Notophthalmus viridescens limb-derived A1 cells (Ferretti & Brookes, 1988) and A1ngfp cells (Yun et al., 2015) were cultured as previously described (Yu et al., 2022; Oliveira et al., 2022); in brief, cells were grown on gelatin-coated flasks in MEM (Gibco) supplemented with 2 nM L-glutamine (Gibco), 10 µg/mL insulin (Sigma), 100 U/mL penicillin/streptomycin (Gibco), 10% heat-inactivated FCS (Gibco) and 25% v/v dH₂O. Cells were passaged 1:2 when approaching 70–80% confluence and maintained at 25°C and 2% CO₂.

4.4 | Induction of differentiation and dedifferentiation

A1 cells were used to generate myotubes. Cells were seeded into gelatin-coated wells at high density (2×10^4 cells/cm²) and subsequently cultured for 5 days in culture media with 0.25% FCS to promote differentiation. To assay cell cycle re-entry, cultures were then exposed to fresh media for 72 h (supplemented with 0.25, 1% or 10% FCS [PAA] as described) containing 5 µM EdU, or with co-culture and conditioned media treatment as described.

4.5 | Senescence induction and conditioned media generation

In vitro senescence induction was performed according to Yu et al. (2023), using UV-irradiation (3 J/m², UV Stratalinker) or 24-h exposure to 20 µM etoposide, both followed by treatment with 1 µM Nutlin-3a. Senescence induction following 12 days' treatment was confirmed by positive SA-β-gal staining, a significant reduction in EdU incorporation, expansion of mitochondrial and lysosomal networks and persistent DNA damage foci (Yu et al., 2022). Control proliferating cells were seeded in parallel, treated only with identical volumes of DMSO and passaged during the 12-day senescence induction to avoid confluence. For co-culture assays, proliferating and senescent cells were harvested, cells were counted using an automated cell counter (Scepter 2.0, Millipore) and seeded into co-culture at a 1:10 ratio to cells initially seeded for myogenesis (i.e., 2×10^3 cells/cm²), mimicking the proportion of senescent cells reported in blastemas in vivo (Yun et al., 2015). For conditioned media treatment, 10 cm plates of proliferating or senescent cells at comparable confluence were washed in 80% PBS ('A-PBS'), before incubation with 10 mL fresh media for 48 h. Conditioned media was subsequently collected and passed

through a 0.22 µm filter prior to use. Fresh conditioned media was used in every experiment.

4.6 | Inhibitor treatments

Drug toxicity assessment was performed by seeding cells into 96-well plates before subsequent treatment with a dose curve of each inhibitor (Table S1) for 72 h. Cell viability was then assessed using the alamarBlue assay according to manufacturer's instructions. For small molecules used in dedifferentiation assays, drug doses selected maintained >80% of control cell viability by alamarBlue assessment (data not shown). For ABT263 and dasatinib senolytic assessment, control proliferating and senescent cells were assessed in parallel.

4.7 | EdU, SA-β-gal and immunostaining

SA-β-gal staining was performed according to manufacturer's instructions (Cell Signalling) as described (Yun et al., 2015), prior to permeabilisation, EdU or immunostaining procedures. Click-iT EdU staining was performed according to manufacturer's instructions (Invitrogen); in brief, cultures were fixed in 4% PFA at 4°C for 10–15 min, permeabilised with 0.2% Triton-X100 in PBS and stained with the Click-iT reaction cocktail. Prior to immunostaining, samples were blocked in 10% goat serum in PBS for >30 min (RT), and immunostaining was performed (see Table S2 for details of antibodies used). Primary antibodies were incubated overnight at 4°C and secondary antibodies for 1–4 h at room temperature. Antibodies were diluted in 5% goat serum and 0.1% Triton-X100 in PBS, and samples were washed twice in PBS between primary and secondary incubation. Nuclei were counterstained using Hoechst 33342.

4.8 | Imaging

Imaging of in vitro fluorescence experiments was performed using a Nikon Eclipse TsER microscope. A Zeiss AxioZoom V16 microscope was used to perform SA-β-gal imaging. FIJI was used for image analysis. Imaging of in vivo dedifferentiation experiments was conducted using a Zeiss AxioZoom V.16 fluorescence stereomicroscope and Zen software (Zeiss). For each sample, 10 sections were scored. Blind counting was employed for all quantifications.

4.9 | Western blotting

For western blotting, myotube cultures were lysed in situ using 0.02 M Hepes (pH 7.9), 0.2 mM EDTA, 1.5 mM MgCl₂, 0.42 M NaCl, 25% glycerol lysis buffer, incubated for 30 min at 4°C and subsequently cleared of debris by centrifugation. Protein concentration was analysed by the Bradford assay, and denatured lysates of equal protein amount were loaded onto 10% Bis-Tris Novex gels and run



at 150V for 1h in MOPS-SDS running buffer. Overnight transfer onto nitrocellulose membranes was performed in methanol transfer buffer, before membranes were blocked (Odyssey blocking buffer, Licor, 30min RT) and probed with primary antibodies in blocking buffer (>1h), before washing in PBS-T and probing with secondary antibodies. Blots were thoroughly washed in PBS and scanned using an Odyssey scanner (Licor). Bands were quantified from triplicate samples against loading controls using FIJI.

4.10 | RNAseq

For myotube purification, cultures were washed gently with A-PBS, lifted using trypsin and then quenched using fresh media. Cell suspensions were passed sequentially through 100µm filters (to exclude aggregates) and 35µm filters. Myotubes retained on the 35µm filters were collected in fresh media and spun down. Proliferating and senescent mononucleate cultures were not filtered, but were simply lifted and spun down. Myotube or cell pellets were immediately lysed in buffer RLT and RNA extracted using RNeasy mini (mononucleate) or micro (myotube) kits according to manufacturer's instructions. cDNA synthesis and RNA sequencing was subsequently performed by the Dresden Concept Genome Center (DCGC). For bioinformatic analysis, [useGalaxy.org](https://usegalaxy.org) (Afgan et al., 2018) was used for initial processing. Firstly, adapter sequences were trimmed from FASTQ files using TrimGalore, quality control performed using FastQC. Alignment of trimmed reads to the *N.viridescens* transcriptome (Abdullayev et al., 2013) was performed using Sailfish. Data were then imported into Rstudio for normalisation and differential gene expression analysis using DESeq2 with a significance cut-off of $p < 0.05$.

4.11 | Statistical analysis

Statistical analysis was performed using Prism software; for comparison of $n > 2$ sample groups, ANOVA and post hoc Dunnett or Tukey tests were performed, and for comparison of $n = 2$ sample groups, two-tailed student *t* tests were applied as described.

AUTHOR CONTRIBUTIONS

HEW, KET, AG and MHY designed and performed experiments, analysed and interpreted data. HEW wrote the article with input from all authors. HEW and MHY acquired funding. MHY supervised the study.

ACKNOWLEDGMENTS

We thank Heng Wang for the donation of lineage-tracing plasmids and technical advice, the Dresden Concept Genome Centre (CRTD, TU Dresden) for performing RNAseq, Phillip Gates for technical support and all members of Yun lab for advice and comments on the article. HEW was supported by an Alexander von Humboldt postdoctoral research fellowship and a TU Dresden Graduate Academy 'Postdoc Starter Kit' grant. KET is supported by a DAAD Scholarship. AG is

part of the FSJ programme at CRTD. MHY is supported by Deutsche Forschungsgemeinschaft grants (DFG 22137416, 450807335 and 497658823) and TUD-CRTD core funds. Open Access funding enabled and organized by Projekt DEAL.

CONFLICT OF INTEREST STATEMENT

The authors declare no competing interests.

DATA AVAILABILITY STATEMENT

The data that support the findings of this study are openly available in the GEO repository at [<https://www.ncbi.nlm.nih.gov/geo/query/acc.cgi?acc=GSE211798>], reference number [GSE211798].

ORCID

Maximina H. Yun  <https://orcid.org/0000-0001-9019-2453>

REFERENCES

- Abdullayev, I., Kirkham, M., Björklund, Å. K., Simon, A., & Sandberg, R. (2013). A reference transcriptome and inferred proteome for the salamander *Notophthalmus viridescens*. *Experimental Cell Research*, 319(8), 1187–1197. <https://doi.org/10.1016/j.yexcr.2013.02.013>
- Acosta, J. C., O'Loughlin, A., Banito, A., Guijarro, M. V., Augert, A., Raguz, S., Fumagalli, M., da Costa, M., Brown, C., Popov, N., Takatsu, Y., Melamed, J., d'Adda di Fagnana, F., Bernard, D., Hernando, E., & Gil, J. (2008). Chemokine signaling via the CXCR2 receptor reinforces senescence. *Cell*, 133(6), 1006–1018. <https://doi.org/10.1016/j.cell.2008.03.038>
- Afgan, E., Baker, D., Batut, B., van den Beek, M., Bouvier, D., Cech, M., Chilton, J., Clements, D., Coraor, N., Gruning, B. A., Guerler, A., Hillman-Jackson, J., Hiltmann, S., Jalili, V., Rasche, H., Soranzo, N., Goecks, J., Taylor, J., Nekrutenko, A., & Blankenberg, D. (2018). The galaxy platform for accessible, reproducible and collaborative biomedical analyses: 2018 update. *Nucleic Acids Research*, 46(W1), W537–W544. <https://doi.org/10.1093/nar/gky379>
- Baker, D. J., Childs, B. G., Durik, M., Wijers, M. E., Sieben, C. J., Zhong, J., Saltness, R. A., Jeganathan, K. B., Verzosa, G. C., Pezeshki, A., Khazaie, K., Miller, J. D., & van Deursen, J. (2016). Naturally occurring p16Ink4a-positive cells shorten healthy lifespan. *Nature*, 530(7589), 184–189. <https://doi.org/10.1038/nature16932>
- Banito, A., Rashid, S. T., Acosta, J. C., Li, S., Pereira, C. F., Geti, I., Pinho, S., Silva, J. C., Azuara, V., Walsh, M., Vallier, L., & Gil, J. (2009). Senescence impairs successful reprogramming to pluripotent stem cells. *Genes & Development*, 23(18), 2134–2139. <https://doi.org/10.1101/gad.1811609>
- Bussian, T. J., Aziz, A., Meyer, C. F., Swenson, B. L., van Deursen, J. M., & Baker, D. J. (2018). Clearance of senescent glial cells prevents tau-dependent pathology and cognitive decline. *Nature*, 562(7728), 578–582. <https://doi.org/10.1038/s41586-018-0543-y>
- Campisi, J. (2013). Aging, cellular senescence, and cancer. *Annual Review of Physiology*, 75(1), 685–705. <https://doi.org/10.1146/annurev-physiol-030212-183653>
- Chiche, A., Le Roux, I., von Joest, M., Sakai, H., Aguin, S. B., Cazin, C., Salam, R., Fiette, L., Alegria, O., Flamant, P., Tajbakhsh, S., & Li, H. (2017). Injury-induced senescence enables in vivo reprogramming in skeletal muscle. *Cell Stem Cell*, 20(3), 407–414. <https://doi.org/10.1016/j.stem.2016.11.020>
- Childs, B. G., Baker, D. J., Wijshake, T., Conover, C. A., Campisi, J., & van Deursen, J. M. (2016). Senescent intimal foam cells are deleterious at all stages of atherosclerosis. *Science*, 354(6311), 472–477. <https://doi.org/10.1126/science.aaf6659>



- Chuprin, A., Gal, H., Biron-Shental, T., Biran, A., Amiel, A., Rozenblatt, S., & Krizhanovsky, V. (2013). Cell fusion induced by ERVWE1 or measles virus causes cellular senescence. *Genes & Development*, 27(21), 2356–2366. <https://doi.org/10.1101/gad.227512.113>
- Coppé, J.-P., Patil, C. K., Rodier, F., Sun, Y., Muñoz, D. P., Goldstein, J., Nelson, P. S., Desprez, P. Y., & Campisi, J. (2008). Senescence-associated secretory phenotypes reveal cell-nonautonomous functions of oncogenic RAS and the p53 tumor suppressor. *PLoS Biology*, 6(12), 2853–2868. <https://doi.org/10.1371/journal.pbio.0060301>
- Cox, B. D., Yun, M. H., & Poss, K. D. (2019). Can laboratory model systems instruct human limb regeneration? *Development*, 146(20), dev181016. <https://doi.org/10.1242/dev.181016>
- Currie, J. D., Kawaguchi, A., Traspas, R. M., Schuez, M., Chara, O., & Tanaka, E. M. (2016). Live imaging of axolotl digit regeneration reveals spatiotemporal choreography of diverse connective tissue progenitor pools. *Developmental Cell*, 39(4), 411–423. <https://doi.org/10.1016/j.devcel.2016.10.013>
- Da Silva-Álvarez, S., Guerra-Varela, J., Sobrido-Cameán, D., Quelle, A., Barreiro-Iglesias, A., Sánchez, L., & Collado, M. (2020). Cell senescence contributes to tissue regeneration in zebrafish. *Aging Cell*, 19(1), e13052. <https://doi.org/10.1111/accel.13052>
- Davaapil, H., Brockes, J. P., & Yun, M. H. (2016). Conserved and novel functions of programmed cellular senescence during vertebrate development. *Development*, 144, 106–114. <https://doi.org/10.1242/dev.138222>
- Del Rio-Tsonis, K., Trombley, M. T., McMahon, G., & Tsonis, P. A. (1998). Regulation of lens regeneration by fibroblast growth factor receptor 1. *Developmental Dynamics*, 213(1), 140–146. [https://doi.org/10.1002/\(SICI\)1097-0177\(199809\)213:1<140::AID-AJA14>3.0.CO;2-6](https://doi.org/10.1002/(SICI)1097-0177(199809)213:1<140::AID-AJA14>3.0.CO;2-6)
- Demaria, M., Ohtani, N., Youssef, S. A., Rodier, F., Toussaint, W., Mitchell, J. R., Laberge, R. M., Vijg, J., Van Steeg, H., Dollé, M. E., Hoeijmakers, J. H., de Bruin, A., Hara, E., & Campisi, J. (2014). An essential role for senescent cells in optimal wound healing through secretion of PDGF-AA. *Developmental Cell*, 31(6), 722–733. <https://doi.org/10.1016/j.devcel.2014.11.012>
- Ferretti, P., & Brockes, J. P. (1988). Culture of newt cells from different tissues and their expression of a regeneration-associated antigen. *Journal of Experimental Zoology*, 247(1), 77–91. <https://doi.org/10.1002/jez.1402470111>
- García-Prat, L., Martínez-Vicente, M., Perdiguer, E., Ortet, L., Rodríguez-Ubrea, J., Rebollo, E., Ruiz-Bonilla, V., Gutarra, S., Ballestar, E., Serrano, A. L., Sandri, M., & Muñoz-Cánoves, P. (2016). Autophagy maintains stemness by preventing senescence. *Nature*, 534(7607), S3–S4. <https://doi.org/10.1038/nature19415>
- Gerber, T., Murawala, P., Knapp, D., Masselink, W., Schuez, M., Hermann, S., Gac-Santel, M., Nowoshilow, S., Kageyama, J., Khattak, S., Currie, J. D., Camp, J. G., Tanaka, E. M., & Treutlein, B. (2018). Single-cell analysis uncovers convergence of cell identities during axolotl limb regeneration. *Science*, 362(6413), eaq0681. <https://doi.org/10.1126/science.aq0681>
- Horbelt, D., Boergermann, J. H., Chaikuad, A., Alfano, I., Williams, E., Lukonin, I., Timmel, T., Bullock, A. N., & Knaus, P. (2015). Small molecules dorsomorphin and LDN-193189 inhibit myostatin/GDF8 signaling and promote functional myoblast differentiation. *Journal of Biological Chemistry*, 290(6), 3390–3404. <https://doi.org/10.1074/jbc.M114.604397>
- Jeon, O. H., Kim, C., Laberge, R.-M., Demaria, M., Rathod, S., Vasserot, A. P., Chung, J. W., Kim, D. H., Poon, Y., David, N., Baker, D. J., van Deursen, J. M., Campisi, J., & Elisseff, J. H. (2017). Local clearance of senescent cells attenuates the development of post-traumatic osteoarthritis and creates a pro-regenerative environment. *Nature Medicine*, 23(6), 775–781. <https://doi.org/10.1038/nm.4324>
- Joven, A., Elewa, A., & Simon, A. (2019). Model systems for regeneration: salamanders. *Development*, 146(14), dev167700. <https://doi.org/10.1242/dev.167700>
- Jun, J.-I., & Lau, L. F. (2010). The matricellular protein CCN1 induces fibroblast senescence and restricts fibrosis in cutaneous wound healing. *Nature Cell Biology*, 12(7), 676–685. <https://doi.org/10.1038/ncb2070>
- Kong, X., Feng, D., Wang, H., Hong, F., Bertola, A., Wang, F.-S., & Gao, B. (2012). Interleukin-22 induces hepatic stellate cell senescence and restricts liver fibrosis in mice. *Hepatology*, 56(3), 1150–1159. <https://doi.org/10.1002/hep.25744>
- Kostakopoulou, K., Vogel, A., Brickell, P., & Tickle, C. (1996). 'Regeneration' of wing bud stumps of chick embryos and reactivation of Msx-1 and shh expression in response to FGF-4 and ridge signals. *Mechanisms of Development*, 55(2), 119–131. [https://doi.org/10.1016/0925-4773\(95\)00492-0](https://doi.org/10.1016/0925-4773(95)00492-0)
- Krizhanovsky, V., Yon, M., Dickinson, R. A., Hearn, S., Simon, J., Miething, C., Yee, H., Zender, L., & Lowe, S. W. (2008). Senescence of activated stellate cells limits liver fibrosis. *Cell*, 134(4), 657–667. <https://doi.org/10.1016/j.cell.2008.06.049>
- Kuilman, T., Michaloglou, C., Vredeveld, L. C. W., Douma, S., van Doorn, R., Desmet, C. J., Aarden, L. A., Mooi, W. J., & Peeper, D. S. (2008). Oncogene-induced senescence relayed by an interleukin-dependent inflammatory network. *Cell*, 133(6), 1019–1031. <https://doi.org/10.1016/j.cell.2008.03.039>
- Kumar, A., Velloso, C. P., Imokawa, Y., & Brockes, J. P. (2000). Plasticity of retrovirus-labelled myotubes in the newt limb regeneration blastema. *Developmental Biology*, 218(2), 125–136. <https://doi.org/10.1006/dbio.1999.9569>
- Le Roux, I., Konge, J., Le Cam, L., Flamant, P., & Tajbakhsh, S. (2015). Numb is required to prevent p53-dependent senescence following skeletal muscle injury. *Nature Communications*, 6(1), 8528. <https://doi.org/10.1038/ncomms9528>
- Lo, D. C., Allen, F., & Brockes, J. P. (1993). Reversal of muscle differentiation during urodele limb regeneration. *Proceedings of the National Academy of Sciences*, 90(15), 7230–7234. <https://doi.org/10.1073/pnas.90.15.7230>
- Meyer, K., Hodwin, B., Ramanujam, D., Engelhardt, S., & Sarikas, A. (2016). Essential role for premature senescence of myofibroblasts in myocardial fibrosis. *Journal of the American College of Cardiology*, 67(17), 2018–2028. <https://doi.org/10.1016/j.jacc.2016.02.047>
- Milanovic, M., Fan, D. N. Y., Belenki, D., Däbritz, J. H. M., Zhao, Z., Yu, Y., Dörr, J. R., Dimitrova, L., Lenze, D., Monteiro Barbosa, I. A., Mendoza-Parra, M. A., Kanashova, T., Metzner, M., Pardon, K., Reimann, M., Trumpf, A., Dörken, B., Zuber, J., Gronemeyer, H., ... Schmitt, C. A. (2018). Senescence-associated reprogramming promotes cancer stemness. *Nature*, 553(7686), 96–100. <https://doi.org/10.1038/nature25167>
- Mosteiro, L., Pantoja, C., Alcazar, N., Marión, R. M., Chondronasiou, D., Rovira, M., Fernandez-Marcos, P. J., Muñoz-Martin, M., Blanco-Aparicio, C., Pastor, J., Gómez-López, G., De Martino, A., Blasco, M. A., Abad, M., & Serrano, M. (2016). Tissue damage and senescence provide critical signals for cellular reprogramming in vivo. *Science*, 354(6315), aaf4445. <https://doi.org/10.1126/science.aaf4445>
- Mosteiro, L., Pantoja, C., de Martino, A., & Serrano, M. (2018). Senescence promotes in vivo reprogramming through p16^{INK4a} and IL-6. *Aging Cell*, 17(2), e12711. <https://doi.org/10.1111/accel.12711>
- Muñoz-Espín, D., Cañamero, M., Maraver, A., Gómez-López, G., Contreras, J., Murillo-Cuesta, S., Rodríguez-Baeza, A., Varela-Nieto, I., Ruberte, J., Collado, M., & Serrano, M. (2013). Programmed cell senescence during mammalian embryonic development. *Cell*, 155(5), 1104–1118. <https://doi.org/10.1016/j.cell.2013.10.019>
- Oliveira, C. R., Knapp, D., Elewa, A., Gerber, T., Gonzalez Malagon, S. G., Gates, P. B., Walters, H. E., Petzold, A., Arce, H., Cordoba, R. C., Subramanian, E., Chara, O., Tanaka, E. M., Simon, A., & Yun, M. H. (2022). Tg1 regulates proximo-distal identity during salamander limb regeneration. *Nature Communications*, 13(1), 1141. <https://doi.org/10.1038/s41467-022-28755-1>



- Poss, K. D., Shen, J., Nechiporuk, A., McMahon, G., Thisse, B., Thisse, C., & Keating, M. T. (2000). Roles for Fgf signaling during zebrafish fin regeneration. *Developmental Biology*, 222(2), 347–358. <https://doi.org/10.1006/dbio.2000.9722>
- Ratnayake, D., Nguyen, P. D., Rossello, F. J., Wimmer, V. C., Tan, J. L., Galvis, L. A., Julier, Z., Wood, A. J., Boudier, T., Isiaku, A. I., Berger, S., Oorschot, V., Sonntag, C., Rogers, K. L., Marcelle, C., Lieschke, G. J., Martino, M. M., Bakkers, J., & Currie, P. D. (2021). Macrophages provide a transient muscle stem cell niche via NAMPT secretion. *Nature*, 591(7849), 281–287. <https://doi.org/10.1038/s41586-021-03199-7>
- Ritschka, B., Storer, M., Mas, A., Heinzmann, F., Ortells, M. C., Morton, J. P., Sansom, O. J., Zender, L., & Keyes, W. M. (2017). The senescence-associated secretory phenotype induces cellular plasticity and tissue regeneration. *Genes & Development*, 31(2), 172–183. <https://doi.org/10.1101/gad.290635.116>
- Sandoval-Guzmán, T., Wang, H., Khattak, S., Schuez, M., Roensch, K., Nacu, E., Tazaki, A., Joven, A., Tanaka, E. M., & Simon, A. (2014). Fundamental differences in dedifferentiation and stem cell recruitment during skeletal muscle regeneration in two salamander species. *Cell Stem Cell*, 14(2), 174–187. <https://doi.org/10.1016/j.stem.2013.11.007>
- Satoh, A., Makanae, A., Nishimoto, Y., & Mitogawa, K. (2016). FGF and BMP derived from dorsal root ganglia regulate blastema induction in limb regeneration in *Ambystoma mexicanum*. *Developmental Biology*, 417(1), 114–125. <https://doi.org/10.1016/j.ydbio.2016.07.005>
- Storer, M., Mas, A., Robert-Moreno, A., Pecoraro, M., Ortells, M. C., Di Giacomo, V., Yosef, R., Pilpel, N., Krizhanovsky, V., Sharpe, J., & Keyes, W. M. (2013). Senescence is a developmental mechanism that contributes to embryonic growth and patterning. *Cell*, 155(5), 1119–1130. <https://doi.org/10.1016/j.cell.2013.10.041>
- Takeo, M., Chou, W. C., Sun, Q., Lee, W., Rabbani, P., Loomis, C., Taketo, M. M., & Ito, M. (2013). Wnt activation in nail epithelium couples nail growth to digit regeneration. *Nature*, 499(7457), 228–232. <https://doi.org/10.1038/nature12214>
- Tanaka, E. M., Drechsel, D. N., & Brockes, J. P. (1999). Thrombin regulates S-phase re-entry by cultured newt myotubes. *Current Biology*, 9(15), 792–799. [https://doi.org/10.1016/S0960-9822\(99\)80362-5](https://doi.org/10.1016/S0960-9822(99)80362-5)
- Tanaka, E. M., Gann, A. A. F., Gates, P. B., & Brockes, J. P. (1997). Newt myotubes reenter the cell cycle by phosphorylation of the retinoblastoma protein. *Journal of Cell Biology*, 136(1), 155–165. <https://doi.org/10.1083/jcb.136.1.155>
- Tsonis, P. A. (2006). How to build and rebuild a lens. *Journal of Anatomy*, 209(4), 433–437. <https://doi.org/10.1111/j.1469-7580.2006.00634.x>
- Wagner, I., Wang, H., Weissert, P. M., Straube, W. L., Shevchenko, A., Gentzel, M., Brito, G., Tazaki, A., Oliveira, C., Sugiyama, T., Shevchenko, A., Simon, A., Drechsel, D. N., & Tanaka, E. M. (2017). Serum proteases potentiate BMP-induced cell cycle re-entry of dedifferentiating muscle cells during newt limb regeneration. *Developmental Cell*, 40(6), 608–617. <https://doi.org/10.1016/j.devcel.2017.03.002>
- Walters, H. E., & Yun, M. H. (2020). Rising from the ashes: Cellular senescence in regeneration. *Current Opinion in Genetics & Development*, 64, 94–100. <https://doi.org/10.1016/j.gde.2020.06.002>
- Wang, H., Löff, S., Borg, P., Nader, G. A., Blau, H. M., & Simon, A. (2015). Turning terminally differentiated skeletal muscle cells into regenerative progenitors. *Nature Communications*, 6(1), 7916. <https://doi.org/10.1038/ncomms8916>
- Wang, H., & Simon, A. (2016). Skeletal muscle dedifferentiation during salamander limb regeneration. *Current Opinion in Genetics & Development*, 40, 108–112. <https://doi.org/10.1016/j.gde.2016.06.013>
- Yun, M. H., Davaapil, H., & Brockes, J. P. (2015). Recurrent turnover of senescent cells during regeneration of a complex structure. *eLife*, 4, e05505. <https://doi.org/10.7554/eLife.05505>
- Yun, M. H., Gates, P. B., & Brockes, J. P. (2013). Regulation of p53 is critical for vertebrate limb regeneration. *Proceedings of the National Academy of Sciences*, 110(43), 17392–17397. <https://doi.org/10.1073/pnas.1310519110>
- Yu, Q., Walters, H. E., Pasquini, G., Singh, S. P., León-Perián, D., Petzold, A., Kesavan, P., Subiran, C., Garteizgogea, I., Knapp, D., Wagner, A., Bernardos, A., Alfonso, M., Nadar, G., Dahl, A., Busskamp, V., Martínez-Máñez, R., & Yun, M. H. (2022). Cellular senescence modulates progenitor cell expansion during axolotl limb regeneration. *bioRxiv*. <https://doi.org/10.1101/2022.09.01.506196>
- Yu, Q., Walters, H. E., & Yun, M. H. (2023). Induction and characterization of cellular senescence in salamanders. *Methods in Molecular Biology*, 2562, 135–154. https://doi.org/10.1007/978-1-0716-2659-7_8
- Yun, M. H., Gates, P. B., & Brockes, J. P. (2014). Sustained ERK activation underlies reprogramming in regeneration-competent salamander cells and distinguishes them from their mammalian counterparts. *Stem Cell Reports*, 3(1), 15–23. <https://doi.org/10.1016/j.stemcr.2014.05.009>
- Zhao, Y., Tyshkovskiy, A., Muñoz-Espín, D., Tian, X., Serrano, M., de Magalhães, J. P., Nevo, E., Gladyshev, V. N., Seluanov, A., & Gorbunova, V. (2018). Naked mole rats can undergo developmental, oncogene-induced and DNA damage-induced cellular senescence. *Proceedings of the National Academy of Sciences*, 115(8), 1801–1806. <https://doi.org/10.1073/pnas.1721160115>

SUPPORTING INFORMATION

Additional supporting information can be found online in the Supporting Information section at the end of this article.

How to cite this article: Walters, H. E., Troyanovskiy, K. E., Graf, A. M., & Yun, M. H. (2023). Senescent cells enhance newt limb regeneration by promoting muscle dedifferentiation. *Aging Cell*, 22, e013826. <https://doi.org/10.1111/ace1.13826>